Quantifying surface water-groundwater exchange using temperature profile inverse modeling at a riparian wetland

Jack Lange

May 2018

Acknowledgments

Abstract

Second Creek is a manoomin (wild rice) stream located on the Iron Range in northeast Minnesota that has been impacted by mining pollution. In order to understand how mining-derived sulfate affects biogeochemical cycling at Second Creek, surface water-ground water exchange must be quantified because it controls geochemical gradients in the sediment. We employed inverse temperature profile modeling to estimate hyporheic flux (groundwater – surface water exchange) at the site. The Second Creek study site is a riparian wetland where low hyporheic flux is expected. Streambed temperature profiles were measured at three locations across a transect of the site spanning from the main stream channel to the flanking wetland area over the summer of 2016. The data were collected using low-cost, open-source vertical temperature profilers and "ALog" data loggers. The USGS model 1DTempPro was applied to the temperature data, along with colocated head data to estimate hydraulic conductivity across the transect. The sediment thermal parameters used in the model were constrained based on the sediment bulk density, which is strongly controlled by soil organic content. The estimated hydraulic conductivity values were applied to the measured head gradients to generate time series of hyporheic flux at each probe for the summer. Results showed spatial variability in both hydraulic properties and hyporheic flux. Across the transect, flux was upward toward the surface water for nearly the entire summer, though the magnitude of the flux varied dynamically in response to variable weather conditions and one flux reversal occurred following a strong late-summer storm event.

Table of Contents

Introduction

Mining in Minnesota's Iron Range impacts water quality in the region. Elevated sulfate concentrations are present in the lakes and streams of the area due to runoff from mining operations. Concern that elevated sulfate levels in the surface water would negatively impact manoomin (wild rice) growth has prompted in depth studies of geochemical processes in aquatic ecosystems in the region (Myrbo et al., 2017a; Myrbo et al., 2017b; Pollman et al., 2017; Pastor et al., 2017; Yourd 2017).

The work in this study is a continuation of the work done by Yourd (2017) and Ng et al. (2017a)) who investigated the effect of hydrologic conditions on sulfur cycling in stream sediment. Their study focused on a stream called Second Creek, which is located in northeastern Minnesota on the Iron Range. More information on the study site is presented in the Study Site section.

This study addresses the need identified in Yourd (2017) for a reliable constraint on hydrologic flux at the Second Creek site. This constraint is necessary because the geochemical gradient in the hyporheic zone where manoomin is rooted is controlled by hydrologic flux (Hayashi & Rosenberry 2002; Kurtz et al. 2007). The inverse temperature profile modelling technique was employed using data collected in the summer of 2016 to better constrain the hyporheic flux at the site.

Study Site

Figure 1: Second Creek Study Site. Yellow X's indicate the location of each temperature probe and collocated piezometer. From west to east, each location is referred to as the "west wetland", "west streambed", and the "center streambed". The red triangle represents the location of the stream gauge.

The Second Creek site is a riparian wetland. The main stream channel is 2-3 meters wide and surrounded by 20-30 meters of wetland. The main channel is 1-2 meters deep. The site is underlain by glacial outwash and till. At the surface the sediment is heterogeneous and has a high fraction of organic matter. Sources of surface water to the stream include discharge and runoff from mining pits to the north and northeast which cause elevated sulfate levels in the channel (Yourd, 2017). During the summer months, manoomin and submergent macrophytes grow in the

main channel of the stream, and the densely vegetated wetlands contain grasses, sedges, and shrubs (Yourd, 2017).

Methods

The quantity of interest in this study is vertical hydrologic flux in the streambed of Second Creek. Hydrologic flux through porous medium is described by Darcy's law,

$$q_z = -K\frac{dh}{dz},$$ (1)

where q_z is the vertical hydrologic flux, K is the hydraulic conductivity and $\frac{dh}{dz}$ is the gradient of head between the aquifer and the surface water. In hydrologic studies, the head gradient can be directly measured in the field, so the main challenge is quantifying hydraulic conductivity. Hydraulic conductivity is a highly variable quantity that can range over many orders of magnitude. Inverse temperature profile modeling was employed to estimate K so that hydrologic flux can be calculated.

Inverse Temperature Profile Modelling

The inverse temperature profile method uses temperature as a tracer to infer the movement of water through the sediment - surface water interface. In shallow lakes and streams the surface water temperature fluctuates diurnally as it is heated by the sun and subsequently cools overnight. The surface water temperature fluctuation propagates down into the hyporheic zone where the surface water comes into contact with groundwater. The mixing of surface water with relatively constant-temperature groundwater in the streambed attenuates the diurnal temperature signal. In addition to signal attenuation, the signal is also shifted in time because of

7

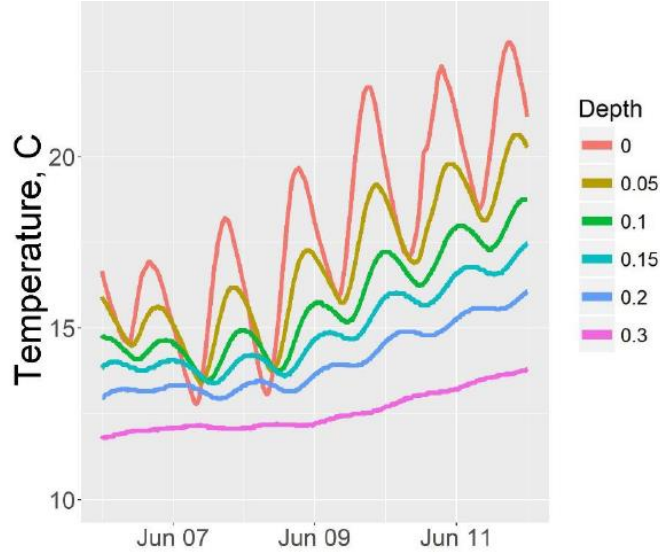the time it takes for the temperature signal to propagate. This phenomenon is demonstrated in Figure 2.

Figure 2: Sample streambed temperature profile from Second Creek. Surface water exhibits the strongest diurnal fluctuations. The diurnal fluctuations are almost entirely damped out at 0.3 m depth. The diurnal signal is also phase shifted at depth.

The magnitude of signal attenuation is related to the direction of water flow in the streambed. In a gaining stream, the signal will damp out at a more shallow depth than in a losing stream, where infiltrating surface water carries the temperature signal with it. The phase lag at depth is controlled by the time over which the signal takes to propagate, which is similarly dictated by hydrologic flux.

One dimensional propagation of heat through a porous medium is well understood and described by the heat diffusion equation:

$$(\lambda_s + q_z \alpha C_w)\frac{\partial^2 T}{\partial t^2} - q_z C_w \frac{\partial T}{\partial z} = \frac{\partial T}{\partial t}(\phi C_w + (1 - \phi)C_s). \qquad (2)$$

The symbols in this equation are defined in Appendix 1.

The inverse temperature profile method uses the top and bottom temperature readings of an observed temperature profile as boundary conditions to predict the full temperature profile using the heat diffusion equation for a given set of parameters. The observed and predicted profiles are then compared. If the match is not good, the parameters, including q_z, can be adjusted. This process can be performed iteratively until the observed and predicted profiles match within a desired error tolerance. The adjustment of the input parameters in this manner allows estimation of the best parameter values for matching observations.

There is a variety of software available to perform inverse temperature profile modeling (Gordon et al., 2011; Koch et al., 2015; Swanson and Cardenas, 2011). The USGS software 1DTempPro (Koch et al., 2015) was chosen for this study because it is the only GUI--based inverse temperature profile modeling software that uses a numerical solution to the heat diffusion equation. Using 1DTempPro, the actual fit of the modeled profile to the temperature data can be evaluated, which is not done with the analytical models. (Koch et al., 2015). 1DTempPro is capable of automated estimation of hydraulic conductivity in a streambed when it is given the physical properties of the streambed, a temperature profile time series, and a collocated head gradient time series. When head data is not available 1DTempPro can be used to estimate the time—average hydrologic flux based on just the physical properties of the streambed and an observed temperature profile. In both of these operational modes all variables except for the variable being estimated are held constant. 1DTempPro uses the iterative Levenberg-Marquardt nonlinear regression method to minimize the residual between the observed and predicted temperature profiles. In this study 1DTempPro was used to estimate hydraulic conductivity at all three temperature probe locations.

9

Data Collection

To estimate hydraulic conductivity, temperature and head data were collected during the summer of 2016. The temperature probes were wooden dowels with 6 thermistors attached. See Figure 3 for a schematic description of the temperature probes.
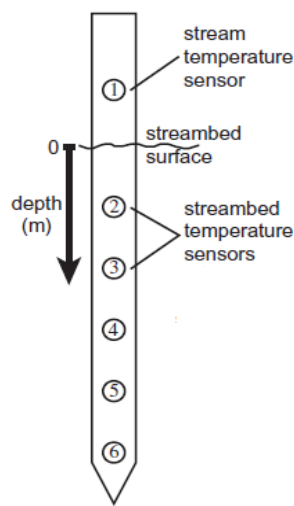
Figure 3: Schematic diagram of a temperature probe.

The probes were inserted into the stream or wetland sediment such that the top thermistor was approximately at the sediment-water interface, and the bottom thermistor was located at approximately 30-40cm depth below the sediment-water interface, with most sensors clustered within the top 10 cm, which corresponds to the manoomin root zone (Yourd, 2017). Temperature readings were logged at 15 minute intervals over 3 to 5 months to capture diurnal and seasonal temperature variability at the site. Two probes collected data from June to August and one collected data from June to October. The location of the probes is indicated in Figure 1.

Head data was collected using three piezometers and a stream gauge. The piezometers and temperature probes were collocated. Pressure transducers in each piezometer and the stream gauge collected pressure data for the entire summer. The data loggers used in this study were low-cost, open-source loggers developed by Northern Widget LLC (Wickert, 2014).

One gap in the stream gauge data exists from 7/25/16 to 8/1/16. The stream gauge went dry during this period. The gauge was relocated in the stream channel during field work on 8/1/2016.

The elevation of the top of casing of each transducer and the stream gauge was surveyed by leveling on 10/1/16. The elevation of each top of casing was measured relative to the top of casing of two permanent monitoring wells on the site. The permanent wells were roughly 120 meters from the transducers and stream gauge. Depth to each transducer was also measured.

Atmospheric pressure data was measured using Schlumberger barologgers. Site precipitation data was acquired from the nearest weather station located in Embarrass, MN, 10 miles north of the site. The precipitation data was accessed via the Midwestern Regional Climate Center cli-MATE database.

The atmospheric pressure was subtracted from the pressure readings made in each piezometer and the stream gauge. The elevation of each transducer was calculated from the surveyed elevation and measured depth for each transducer. The elevation of each transducer was used to convert the pressure measurements into hydraulic head measurements based on a consistent datum across all of the piezometers.

The elevation of the stream gauge was not surveyed before it was moved on 8/1/16, so a correction factor was applied to the head gradient between the stream gauge and each piezometer

11

for the first half of summer. The shift factor was calculated as follows. First 1DTempPro was used to estimate the time--average hydrologic flux at the west streambed probe using the temperature data from the period of time before the stream gauge was moved (the first half of the summer). Then, 1DTempPro was used to estimate the hydraulic conductivity at the west streambed probe location using the temperature and head data that was collected after the stream gauge was moved. The estimated time—average hydraulic flux estimate is independent of the head gradient time series so dividing the average hydraulic flux estimate for the first half of the summer by the hydraulic conductivity estimate for the second half of the summer gives an expected average value for the head gradient during the first half of the summer. The measured head gradient for each piezometer during the first half of the summer was uniformly shifted by the difference between the average of the measured head gradient at the west streambed probe, and the expected average value of the west streambed probe.

Model input parameter estimation

To generate the predicted temperature profile using the heat diffusion equation 1DTempPro requires information about the physical properties of the streambed: porosity, thermal conductivity, and saturated heat capacity. Porosity was previously measured in Myrbo (2013). The remaining physical properties were estimated based on methods in Farouki (1986). The streambed is composed of a mixture of siliciclastic sediments and organic matter (SOM). The sediment at Second Creek is heterogeneous, as show in Figure 4.

Figure 4: Second Creek wetland sediment (left) and streambed sediment (center, right).

(Yourd, 2017)

To make a reasonable estimation of the thermal parameters of the site sediment some simplifying assumptions were required. The first simplifying assumption was that the sediment was composed entirely of two end-members, siliciclastic material and soil organic matter. The second simplifying assumption is that the sediment thermal properties are homogeneous across all of the temperature probe locations. This assumption is necessary because there is not sufficient information to uniquely quantify the sediment composition at each temperature probe. Both of these assumptions are justified during model sensitivity analysis in the results and conclusions section.

The fractions, by mass, of soil organic matter and siliciclastic minerals present in the sediment (x_{si}, $and\ x_{som}$ respectively) were solved for using the following expressions

$$\rho_b = x_{si}\rho_{si} + x_{som}\rho_{som} \tag{3}$$

$$1 = x_{si} + x_{som} \tag{4}$$

13

The value for dry bulk density (ρ_b) of sediment at the site was previously found by Myrbo (2013). Representative values for ρ_{si} and ρ_{som} were sourced from Farouki (1986) who provides typical values for sediment physical and thermal properties. The result of this calculation indicated a sediment makeup of 90% SOM and 10% siliciclastic material. High organic content is expected at Second Creek, and this result is supported by the images above where many of the sediment samples clearly contain significant organic material. The image above also indicate that there are areas at the site where the fraction of SOM in the sediment is less than 90%. To account for this variability an 80% SOM - 20% siliciclastic distribution was used to calculate the thermal properties at the site.

Using the fraction of SOM and siliciclastic material, the thermal properties of the streambed can be estimated by the following methods from Farouki (1986).

Sediment Thermal conductivity, λ

$$\lambda_{max} = x_{Si}\lambda_{Si} + x_{Som}\lambda_{Som} \tag{5}$$

$$\frac{1}{\lambda_{min}} = \frac{x_{Si}}{\lambda_{Si}} + \frac{x_{Som}}{\lambda_{Som}} \tag{6}$$

Saturated heat capacity, C

$$C_{max} = (1-\varphi)x_{Si}C_{Si} + (1-\varphi)x_{Som}C_{Som} + \varphi C_{H_2O} \tag{7}$$

$$C_{min} = \frac{(1-\varphi)x_{Si}}{C_{Si}} + \frac{(1-)x_{Som}}{C_{Som}} + \frac{\varphi}{C_{H_2O}} \tag{8}$$

14

This method bounds the thermal parameter with an upper and lower limit. Values for $\lambda_{Si}, \lambda_{Som}, C_{Si}, C_{Som}$ and C_{H_2O} were found in Farouki (1986). Validity of the resulting parameter range is discussed in the sensitivity analysis portion of the results and conclusions section.

The last parameter needed for predicting the temperature profile is dispersivity. In our study dispersion is the component of heat transfer due to the porous nature of the streambed. Dispersivity empirically relates porewater velocity to dispersion. A range of dispersivity values were considered based on Zheng & Bennet (2002) which provided characteristic dispersivity values for studies performed over a range of scales from tens of centimeters to many kilometers. The validity of the range is analyzed in the sensitivity analysis portion of the results and conclusions section.

Results and Conclusions

The estimates of hydraulic conductivity at each temperature probe location were obtained using 1DTempPro. They are presented in Table 1. The user specified parameter values for these estimations are presented in Table 2. The confidence of the estimated hydraulic conductivity values is explored in the sensitivity analysis section.

Location	Hydraulic conductivity, m/d
West wetland	0.07
Stream west	0.04
Stream center	0.18

Parameter	Value
φ	0.51
λ	0.56 W/(m*C)
C	2.44*10^6 J/(m^3 *C)
α	0.1 m

Table 1: Hydraulic conductivity estimates from the 1DTempPro inverse model. Mode inputs include head and temperature time series and the parameter values in Table 2.

Table 2: 1DTempPro inverse model inputs for hydraulic conductivity estimation.

These hydraulic conductivity values were implemented in Darcy's law with the head gradient time series for each probe to generate a time series of vertical hydrologic flux at each location. The hydrologic flux time series are presented in Figure 5. The time series are plotted with precipitation data from the Embarrass, MN weather station to investigate the relationship between precipitation and hydrologic flux.
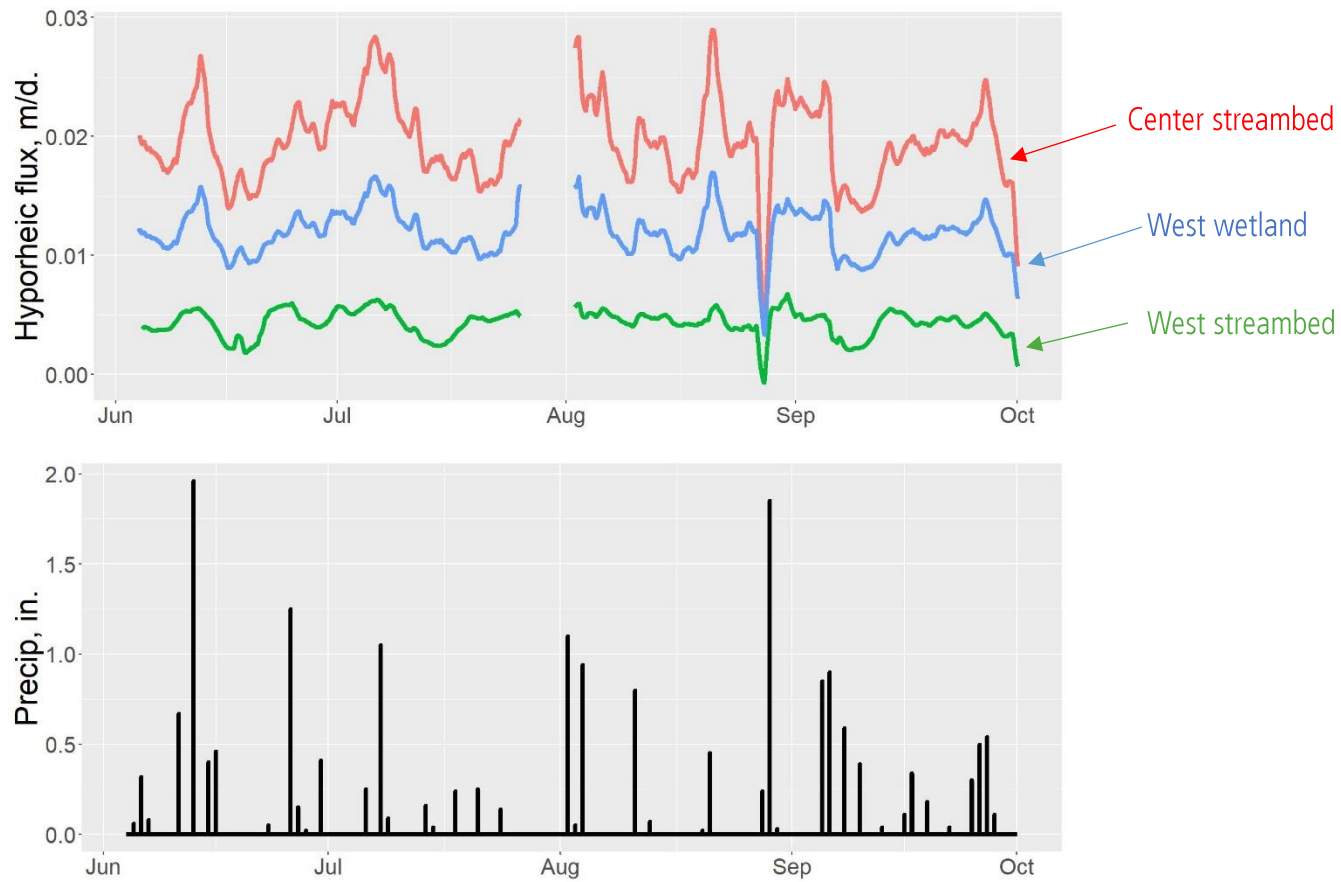
Figure 5: Vertical hyporheic flux and precipitation at Second Creek for summer 2016. Positive values indicate upwards flux of groundwater into the stream. Large storm events appear to control hydrologic flux at the site, though the exact mechanism is uncertain.

The highest hydraulic conductivity and flux occur in center of the stream channel, followed by the west wetland and the west stream channel. This is counterintuitive, as we originally expected the wetland area to have the smallest flux because the wetland sediment generally had higher organic content which we believed to be less hydraulically conductive. There are several possible explanations for this discrepancy. First, the site sediment is highly heterogeneous which suggests that the hydrologic properties are equally heterogeneous. It is possible that the wetland temperature probe was placed in a region that facilitated higher flux

while the west stream probe was located in lower flux regions. Another possible explanation is that flow at the wetland probe has a significant horizontal component, violating the assumption of 1DTempPro that hydrologic flux is entirely in the vertical direction. This explanation has merit because the head in the wetland sediment was consistently higher than the head at the base of the stream which suggests that the water in the wetland sediment could have a significant component of flow towards the stream.

The direction of vertical flux across the transect is upwards for the entire summer except for one brief flux reversal in late August. The magnitude of vertical hydrologic flux over the summer is variable. The flux magnitude appears to be broadly linked with precipitation. Major changes in flux magnitude occur following large rain events. Sometimes these rain events increase the upward flux magnitude, indicating that the rainfall initiates a base flow event. In other cases, rain events are followed by decreased upwards flux, or even downwards flux, indicating that the rainfall elevates the level of surface water. A possible explanation for this discrepancy is that the precipitation data was collected from a weather station that is 10 miles north of the study site so it is possible that during storm events the stream and the weather station don't experience the same meteorological conditions. The stream's response to the storms could be related to the proximity of the storm to the stream. For example, a distant storm would be more likely to trigger a large prolonged base flow event, and a storm that occurs near Second Creek could cause a rapid rise in surface water levels, resulting in an immediate decrease in upwards flux or even downwards flux. Another possible explanation for the varied response to storm events could be seasonal changes in vegetation and evaporation conditions. During the spring evapotranspiration near the stream is lower than in late summer. Following a late summer storm event, evapotranspiration near the stream could lower the head in the subsurface causing

vertical hydrologic flux to decrease or even reverse direction. More study is required to determine which of these explanations have merit.

Sensitivity analysis

This section is dedicated to evaluating the quality of the model results and the model's sensitivity to the thermal parameters calculated using the method of Farouki (1986). To investigate this sensitivity the inverse model was run over the possible range of parameters estimated for dispersivity, thermal conductivity, and heat capacity. The inverse model was run as each parameter was varied over its range while the rest of the parameters were held at the values in Table 2. The resulting value of K for each of these model runs is presented in Figure 6. The mismatch between the model's final predicted profile and the observed temperature profile is qualitatively demonstrated by the size of each point in Figure 6 (larger points indicate larger mismatch). Model mismatch was evaluated using the root mean squared error (RMSE) between each observation and the synthetic temperature profile. For these trials the RMSE ranged from 0.087 degrees to 0.179 degrees. The RMSE for each model run is available in Appendix 2.
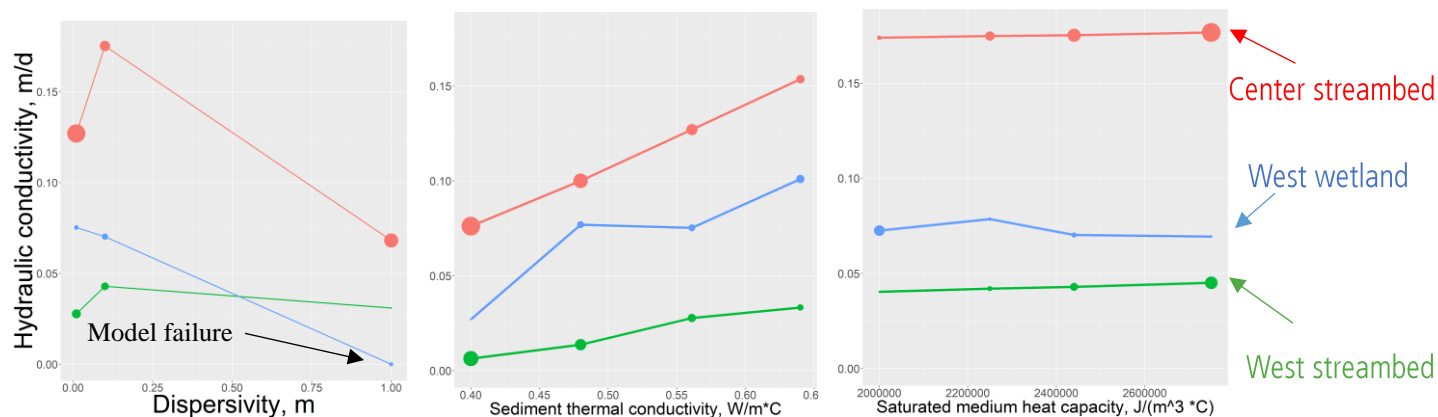

Figure 6: Inverse model sensitivity analysis results. The sensitivity of each hand estimated parameter was tested by running the inverse model over a range of input values and comparing

19

the results. Larger points indicate a larger mismatch between the predicted and observed

temperature profile. Model mismatch was evaluated using the root mean squared error (RMSE)

between each observation and the synthetic temperature profile. RMSE for each model run is

available in Appendix 2.

Dispersivity sensitivity

The inverse model sensitivity results show the strongest nonlinearity in the sensitivity to

dispersivity. This nonlinearity can be explained by the complicated interdependence of

dispersivity and flux magnitude. In Equation 2 the term that represents the transport of heat by

dispersion is

$$q_z \alpha C_w \frac{\partial^2 T}{\partial t^2}. \tag{9}$$

This term shows that the effect of dispersion grows both as hydrologic flux grows and as the

dispersivity, α, grows. The sensitivity analysis shows that low flow velocity (and thus low

hydraulic conductivity) is required to match the observed profile when dispersivity is high. When

dispersivity is lower, higher flux (and thus higher hydraulic conductivity) is required to match

the observed profile.

This relationship does not appear to be linear, however these data are not sufficient to

fully resolve the nonlinear relationship. The cause of this nonlinearity is the codependence of the

dispersion term on both flux (hydraulic conductivity) and dispersivity. An interested reader is

referred to Rau et al. (2012) for further investigation of the significance of thermal dispersion in

heat transport.

The value of dispersivity also depends on the spatial scale over which heat transport is taking place. (Zheng & Bennett, 2002). Zheng & Bennet (2002) state that for an investigation on the scale of tens of centimeters, dispersivity is expected to vary between 0.01m and 1m. In this range, $\alpha = 0.1$m gave the best quality of fit between the predicted temperature profiles and the observed profiles, so this value was chosen to be the representative vertical dispersivity at the site.

Thermal conductivity

The dependence of the inverse model results on thermal conductivity is fairly linear. This makes sense at our site because there is primarily upwards hydrologic flux. As thermal conductivity increases, the diurnal surface water signal can propagate further into the streambed. To match the observed temperature profile, upwards hydrologic flux must damp the diurnal signal. Thus, increasing thermal conductivity results in an increased estimated hydraulic conductivity.

The thermal conductivity value 0.56 W/(m*C) was chosen as the representative thermal conductivity of the sediment at the site. This value was chosen because it gave a good fit for all three temperature probes and, being in the middle of the range of possible values, helped average out heterogeneity at the site.

Saturated heat capacity

The inverse model results appear to have no dependence on saturated heat capacity. The saturated heat capacity value that was chosen to be the representative value for the site was 2.44 x 10^6 J/(m^3 C). The lack of sensitivity to this parameter gives us confidence in choosing this as the representative value.

Summary

To summarize our findings, hydrologic flux at the site during the summer of 2016 was consistently upwards with variation in magnitude driven by precipitation. The results of this work have been used with reactive transport modeling to investigate the influence of hyporheic flux on biogeochemical cycling at Second Creek (Ng el al., 2017b).

The results of this investigation could be expanded and improved by doing unique thermal parameter characterization for each temperature probe. This could be achieved by careful sediment sampling and analysis in the field or by employing a multiple parameter estimation routine. This work would help quantify heterogeneity at the site and could provide more precise estimation of hydraulic conductivity across the site.

Appendix 1 – Symbol definitions for equation 2

Symbol	Variable
K	Hydraulic conductivity
φ	Porosity
λ_s	Saturated thermal conductivity
C_s	Sediment heat capacity
C_w	Heat capacity of water
α	Dispersivity
q_z	Hyporheic flux
T	Temperature

Appendix 2 – Quantitative error data for Figure 6

Dispersivity	Location	Hydraulic Conductivity	RMSE
1	west_wetland	0	0.1
0.1	west_wetland	0.07024	0.11279
0.01	west_wetland	0.075296	0.104
1	stream_west	0.030971	0.087764
0.1	stream_west	0.042949	0.12055
0.01	stream_west	0.027788	0.12751
1	stream_center	0.068234	0.15524
0.1	stream_center	0.17529	0.13477
0.01	stream_center	0.12707	0.17784
Saturated Heat Capacity			
2000000	west_wetland	0.072552	0.12769
2250000	west_wetland	0.078617	0.108
2440000	west_wetland	0.07024	0.11279
2750000	west_wetland	0.069419	0.10559
2000000	stream_west	0.040345	0.10308
2250000	stream_west	0.042006	0.11237
2440000	stream_west	0.042949	0.12055
2750000	stream_west	0.045117	0.13326
2000000	stream_center	0.17396	0.11104
2250000	stream_center	0.17487	0.12415
2440000	stream_center	0.17529	0.13477
2750000	stream_center	0.17668	0.15029
Thermal Conductivity			
0.4	west_wetland	0.027026	0.013328
0.48	west_wetland	0.07692	0.10513
0.561	west_wetland	0.075296	0.104
0.64	west_wetland	0.101	0.1283
0.4	stream_west	0.006384	0.24803
0.48	stream_west	0.013715	0.17946
0.561	stream_west	0.027788	0.12751
0.64	stream_west	0.033272	0.095557
0.4	stream_center	0.076159	0.30978
0.48	stream_center	0.10006	0.23742
0.561	stream_center	0.12707	0.17784
0.64	stream_center	0.15364	0.13054

References

1. Farouki, Omar T. *Thermal Properties of Soils*. Tans Tech, 1986.

2. Gordon, R., Lautz, L., Briggs, M., McKenzie, Jeffrey., 2011. Automated calculation of vertical pore-water flux from field temperature time series using the VFLUX method and computer program. *Journal of Hydrology,* 420–421 (2012) 142–158

3. Hayashi, M. & Rosenberry, D.O., 2002. Effects of Ground Water Exchange on the Hydrology and Ecology of Surface Water. *Groundwater*, 40(3), pp.306–316.

4. Healy, R.W. & Ronan, A.D., 1996. Documentation of computer program VS2DH for simulation of energy transport in variably saturated porous media -- modification of the U.S. Geological Survey's computer program VS2DT. Water-Resources Invenstigations Report 96-4230. *U.S. Geological Survey*.

5. Koch, F.W., Voytek, E.B., Day-Lewis, F.D., Healy, R., Briggs, M.A., Werkema, D., and Lane, J.W., Jr., 2015, 1DTempPro V2: New Features for Inferring Groundwater/Surface-Water Exchange, *Groundwater*, doi:10.1111/gwat.12369, 6p.

6. Koch, F.W., Voytek, E.B., Day-Lewis, F.D., Healy, R., Briggs, M.A., Werkema, D., and Lane, J.W., Jr., 2015, 1DTempPro: A program for analysis of vertical one-dimensional (1D) temperature profiles v2.0: U.S. Geological Survey Software Release, 23 July 2015, http://dx.doi.org/10.5066/F76T0JQS.

7. Kurtz, A.M. et al., 2007. The importance of subsurface geology for water source and vegetation communities in Cherokee Marsh, Wisconsin. *Wetlands*, 27(1), pp.189–202.

8. Myrbo, A., 2013. Wild Rice Sulfate Standard Field Surveys 2011, 2012, 2013: Final
    Report. , Submitted to the Minnesota Pollution Control Agency, St. Paul, Minn.
    University of Minnesota.;

9. Myrbo, A., Swain, E. B., Engstrom, D. R., Coleman Wasik, J., Brenner, J., Dykhuizen
    Shore, M., ... & Blaha, G. (2017)(a). Sulfide generated by sulfate reduction is a primary
    controller of the occurrence of wild rice (Zizania palustris) in shallow aquatic
    ecosystems. *Journal of Geophysical Research: Biogeosciences*, 122(11), 2736-2753.

10. Myrbo, A., E. B. Swain, N. W. Johnson, D. R. Engstrom, J. Pastor, B. Dewey, P.
    Monson, J. Brenner, M. Dykhuizen Shore, and E. B. Peters (B). "Increase in nutrients,
    mercury, and methylmercury as a consequence of elevated sulfate reduction to sulfide in
    experimental wetland mesocosms." *Journal of Geophysical Research: Biogeosciences*
    122, no. 11 (2017): 2769-2785.

11. Ng G.-H. C., A.R. Yourd, N.W. Jonson, A.E. Myrbo., 2017, (a) Modelling hydrologic
    controls on sulfur processes in sulfate-impacted wetland and stream sediments. *Journal of
    Geophysical Research: Biogeosciences,* , volume 122, issues 9, 21 August 2017,
    https://doi.org/10.1002/2017JG003822

12. Ng G.-H. C., O'Hara, P., Santelli, C., Rosenfeld, C., Yourd, A., 2017, (b) Evaluating the
    role of sulfur and hyporheic exchange in biogeochemical cycling in riparian wetlands,
    Abstract H12E-05 presented at 2017 Fall Meeting, AGU, New Orleans, Calif., 11-15
    Dec.

13. Pastor, J. et al., 2017. Effects of sulfate and sulfide on the life cycle of Zizania palustris in
    hydroponic and mesocosm experiments. *Ecological Applications*, 27(1), pp.321–336.

14. Pollman, Curtis D., Edward B. Swain, David Bael, Amy Myrbo, Philip Monson, and Marta Dykhuizen Shore. "The Evolution of Sulfide in Shallow Aquatic Ecosystem Sediments: An Analysis of the Roles of Sulfate, Organic Carbon, and Iron and Feedback Constraints Using Structural Equation Modeling." *Journal of Geophysical Research: Biogeosciences 122, no. 11 (2017): 2719-2735.*

15. Rau, G., Andersen, M., Acworth, R. Experimental investigation of the thermal dispersivity term and its significance in the heat transport equation for flow in sediments. *Water Resources Research,* 48, W03511, doi: 10.1029/2011WR011038

16. Swanson, T.E. and M.B. Cardenas. 2011. Ex-Stream: A MATLAB program for calculating fluid flux through sediment–water interfaces based on steady and transient temperature profiles. Computers and Geosciences, 37, no. 10: 1664-1669.Voytek, E.B., Drenkelfuss, A., Day-Lewis, F.D., Healy, R., Lane, Jr., J.W. and Werkema, D. 2013. 1DTempPro: Analyzing temperature profiles for groundwater/surface-water exchange, *Groundwater*, 52, no. 2: 298-302, doi:10.1111/gwat.12051.

17. Voytek, E.B.; Drenkelfuss, Anja; Day-Lewis, F.D.; Healy, Richard; Lane, J.W., Jr.; and Werkema, Dale, 2013, 1DTempPro: Analyzing Temperature Profiles for Groundwater/Surface-water Exchange: *Ground Water*. March 2014, Vol.52(2), pp.298-302

18. Wickert, A 2014. The Alog: inexpensive, Open Source, Automated Data Collection in the Field. *The Bulletin of the Ecological Society of America,* April 2014, https://doi.org/10.1890/0012-9623-95.2.68

19. Yourd, A., 2017**.** *Using reactive transport modeling to link hydrologic flux and root zone geochemistry at Second Creek, a sulfate enriched wild rice stream in northeastern Minnesota, Masters Thesis, University of Minnesota*.;

20. Zheng, Chunmiao, and Gordon D. Bennett. "Applied Contaminant Transport Modeling, 2nd Edition." *Wiley.com*, 5 Feb. 2002, www.wiley.com/WileyCDA/WileyTitle/productCd-0471384771.html.